Chemical Modelling of Calcium Sulphate Phase Equilibria in Multicomponent Electrolyte Solutions

G. Azimi*, V.G. Papangelakis

Department of Chemical Engineering and Applied Chemistry,
University of Toronto, Toronto, ON M5S 3E5, Canada
*Corresponding author. E-mail: ghazal.azimi@utoronto.ca

Abstract

A new database was developed to successfully model the solid and aqueous phase equilibria in a number of hydrometallurgical processes using the Mixed Solvent Electrolyte (MSE) model of the OLI Systems software. In order to validate the predictability of the model developed, a number of experimental measurements were conducted in multicomponent solutions containing $NiSO_4$, H_2SO_4, $MnSO_4$, HCl, etc. from 25 to 90ºC. The developed model accurately predicts the chemistry of calcium sulphate solid formation in the systems studied in this work as well as in multicomponent sulphate-chloride solutions in nickel hydrometallurgical processes. Since it is not practical to measure solubility data under all possible conditions, because of the large number of components involved, the developed model is a valuable tool for assessing calcium sulphate process chemistry for a wide variety of complex aqueous processing solutions.

Introduction

Scaling or precipitation fouling is the formation of a solid layer on equipment surfaces or piping systems. It is a persistent problem encountered in many industrial processes such as oil and gas production, desalination operations, steam generation plants, heat transfer systems, water supply systems, and hydrometallurgical operations.[1] As the scale layer becomes increasingly thicker, it reduces the production capacity and process efficiency because of increased heat transfer resistance, reduction of material flow, corrosion and wearing out of construction materials.

Calcium sulphate occurs widely in nature and is encountered in many industrial processes such as brine evaporation and phosphate fertilizer industries as well as in mineral processing industries using aqueous chemistry (hydrometallurgy). Calcium sulphate scales are deposited almost anywhere calcium and sulphate are together in aqueous solutions due to their relative insolubility and results in fouled reactor walls, impellers and pumps, as well as clogged pipes. The resulting scale even forms at low pH and can be effectively removed only mechanically. In a recent study, the costs for maintenance and calcium sulphate scales removal were estimated between \$6 and \$10 million per year.[2] Calcium sulphate occurs in three forms: dihydrate (or gypsum) ($CaSO_4.2H_2O$), hemihydrate (or bassanite) ($CaSO_4.0.5H_2O$) and anhydrite ($CaSO_4$), depending on the temperature, pH and formation conditions.

Attempting to theoretically model calcium solubility in pure water and in multicomponent electrolyte solutions has been the topic of many previous studies. The solubility of calcium sulphate hydrates is equal to the sum of the molalities of the free calcium ion, Ca^{2+}, and the associated calcium sulphate neutral species, $CaSO_{4(aq)}$. Therefore, the solubility of calcium sulphate hydrates is governed by following equilibria:

$$CaSO_4.nH_2O_{(s)} = Ca^{2+} + SO_4^{2-} + nH_2O \quad (1)$$

$$Ca^{2+} + SO_4^{2-} = CaSO_{4(aq)} \quad (2)$$

where n=0, 0.5, and 2 correspond to anhydrite, hemihydrate and dihydrate, respectively. The thermodynamic equilibrium constants for reactions (1) and (2) are:

$$K_{SP}^{0} = a_{Ca^{2+}} a_{SO_4^{2-}} a_w^{\ n} \tag{3}$$

$$K_a = \frac{a_{CaSO_4(aq)}}{a_{Ca^{2+}} \cdot a_{SO_4^{2-}}} \tag{4}$$

The solubility of calcium sulphate is:

$$S = [Ca]_{total} = m_{Ca^{2+}} + m_{CaSO_4(aq)} \tag{5}$$

where K^0_{sp} is the solubility product, K_a is the association constant of $CaSO_{4(aq)}$, a is the activity of Ca^{2+}, $CaSO_{4(aq)}$ and SO_4^{2-}, and a_w is the activity of water. The activity is calculated as $a=\gamma \cdot m$ where γ is the activity coefficient and m is molality (mol.kg^{-1}). To calculate the solubility of calcium sulphate hydrates, all the above need to be determined.

A review of published modeling studies shows that no previous work has been formally undertaken to study the simultaneous effects of coexisting metal sulphates and chlorides on the solubility of the three $CaSO_4$ phases over a broad temperature and concentration range, particularly in industrial solutions. Most of the previous studies attempted to theoretically model the solubilities of calcium sulphate compounds in water or in ternary and quaternary aqueous solutions containing H_2SO_4, $MgSO_4$, Na_2SO_4, etc.[3-10] Most of these studies assumed complete electrolyte dissociation; however, in multicomponent systems with complex solution chemistries, such as industrial processing solutions, speciation models are necessary.

The purpose of the present work is to develop a chemical model to describe and predict the solubility of calcium sulphate hydrates in multicomponent sulphate and chloride solutions containing LiCl, $NiSO_4$, $Fe_2(SO_4)_3$, $MnSO_4$, H_2SO_4, etc. Such a model would be a valuable tool for developing, optimizing and designing different industrial processes in which unwanted calcium sulphate precipitation may occur. The new model is based on the MSE (Mixed Solvent Electrolyte) model of the OLI Systems software.[11-13]

In this work, a number of experimental measurements were also conducted in multicomponent solutions containing $NiSO_4$, H_2SO_4, $MnSO_4$, HCl, etc. from 25 to 90°C to validate the predictability of the model developed. The model was shown to accurately predict the chemistry of calcium sulphate solid formation in the systems studied in this work. The predictability of the model was also validated in multicomponent sulphate-chloride solutions in nickel hydrometallurgical solutions for which experimental data are available in the literature.[14]

Experiment Procedure

Chemicals

All solutions used in this study were prepared by dissolving reagent grade chemicals directly without further purification. Calcium sulphate dihydrate (gypsum) reagent was from J.T.Baker with 99.4% purity and was used as one of the saturating solid phases. Calcium sulphate anhydrite was also from J.T.Baker with 100% purity and was used as the other saturating solid phase in this work. XRD analysis carried out on both solid phases from the bottle using a Philips PW3719 diffractometer. Result showed 100% gypsum and anhydrite, respectively. No traces of hemihydrate or anhydrite were found in the gypsum solid powder.

Apparatus

The experiments were done using a 1L double layer reaction vessel and heating was provided through a temperature-controlled circulating oil jacket. The reactor slurry was kept suspended by a shaft stirrer. The temperature of the solution was controlled using a thermocouple.

Procedure

A solution of known composition was placed in the reaction vessel with an excess of solid saturating phase. The contents of the reactor were stirred using a stirrer rod. Experiments were started by heating the charged reactor to a known temperature and allowing the reactor to reach steady state. After equilibration, samples were taken by drawing solution into a preheated syringe. Samples were immediately filtered using 0.20 μm Fisher syringe filters and diluted by 5% HNO_3 and were kept in test tubes at room temperature.

The Ca concentration was determined by Inductively Coupled Plasma (ICP-OES) analysis and the solubility of calcium sulphate was obtained as g/L. The saturated filtrate was also used to determine the density of the saturated solution at the experimental temperature using a portable density meter (DMA 35_N) from Anton Paar. The DMA 35_N density meter measures the density of liquids according to the U-tube principle. Samples were filled into the measuring cell using the built-in pipette-style pump. A temperature sensor measures the sample temperature right at the measuring cell. The temperature was also monitored with measured density values.

Equilibrium Time Determination

The equilibrium time in solubility measurements can vary over a wide range from several hours to several days depending on the dissolution rate of solid phase at the applied conditions. In the present study, a conductivity probe was employed to monitor the conductivity of the solution vs. time in order to ensure equilibration. The conductivity of the solution increases by increasing the temperature and concentration. This means that under thermal and chemical equilibrium, conductivity tends to become constant. As well, several kinetic tests were conducted at various temperatures and the results showed that in most cases at least ~24 h was necessary to achieve complete saturation.

Modelling Methodology

Equilibrium Constant

To obtain the equilibrium constant of reactions (1) and (2) at temperature T and pressure P, the standard state chemical potentials of products and reactants are required. These data are widely available in standard thermodynamic compilations. The HKF model, developed by Tanger and Helgeson[15], is embedded in the OLI software to calculate the standard state thermodynamic properties at high temperatures and pressures up to 1000°C and 5kbar. More details are available elsewhere.[16]

Activity Coefficient Model

Activity coefficient is a parameter which accounts for the nonideality (excess property) of electrolyte solutions:

$$\ln \gamma_i = \left(\frac{\partial (G^E / RT)}{\partial n_i} \right)_{T,P,n_{i \neq j}} \tag{6}$$

where n_i is the number of mole of species i and j is any other species. The pursuit of an expression for G^E (excess Gibbs free energy) to calculate γ has been ongoing for decades. Numerous models have been proposed and some of them have been incorporated into commercial software and applied in industry.

In this work, the MSE activity coefficient model embedded in the OLI Systems software is employed to develop the new chemical model for investigating calcium sulphate chemistry in multicomponent electrolyte solutions. The model incorporates formulations for the excess Gibbs energy and standard-state properties coupled with an algorithm for detailed speciation calculations.

In the MSE model, the excess Gibbs free energy consists of three terms:[13]

$$\frac{G^E}{RT} = \frac{G^E_{LR}}{RT} + \frac{G^E_{MR}}{RT} + \frac{G^E_{SR}}{RT} \tag{7}$$

where G^E_{LR} represents the contribution of long-range electrostatic interactions caused by the Coulomb electrostatic forces and mainly describes the direct effect of charge interactions, G^E_{MR} accounts for the middle-range ionic interactions which is a result of indirect effect of charge interactions such as the charge-dipole interactions and charge-induced dipole interactions that are not included in the long-range term, and G^E_{SR} is the short-range contribution term resulting from intermolecular interactions which are identical between non-electrolyte species that is calculated by the UNIQUAC model.

The long-range interaction contribution is obtained from the Pitzer-Debye-Hückel formula expressed as follows:[17]

$$\frac{G^E_{LR}}{RT} = -\left(\sum_i n_i\right)\frac{4A_x I_x}{\rho}\ln\left(\frac{1+\rho\ I_x^{1/2}}{\sum_i x_i[1+\rho\ (I^0_{x,i})^{1/2}]}\right) \tag{8}$$

where the sum is over all species, I_x is the mole fraction-based ionic strength, $I_{x,i}{}^0$ is the ionic strength for a pure component i, i.e., $I_{x,i}{}^0 = 1/2Z_i^2$, ρ is related to the hard-core collision diameter *(ρ=14.0)* and A_x is the Debye-Hückel constant which is given by:

$$A_x = \frac{1}{3}(2\pi N_A d_S)^{1/2}\left(\frac{e^2}{4\pi\varepsilon_0\varepsilon_s k_B T}\right)^{3/2} \tag{9}$$

where d_s and ε_s are the molar density and the dielectric constant for the solvent, respectively. All calculations related to the long-range contribution are handled by the software, and there is no adjustable parameter in the long-range contribution.

The middle-range interaction is the contribution of the indirect effects of the charge interactions to the excess Gibbs energy. This term can be calculated from an ionic-strength dependent, second coefficient-type expression as follows:

$$\frac{G^E_{MR}}{RT} = -\left(\sum_i n_i\right)\sum_i\sum_j x_i x_j B_{ij}(I_x) \tag{10}$$

where x is the mole fraction of species, and B_{ij} is a binary interaction parameter between species i and j (ion or molecule) and is similar to the second virial coefficient, which is a function of ionic strength according to the following equations:

$$B_{ij}(I_x) = b_{ij} + c_{ij}.\exp(-\sqrt{I_x + 0.01}) \qquad (B_{ij} = B_{ji}) \tag{11}$$

In general, the parameters b_{ij} and c_{ij} are calculated as functions of temperature as following:

$$b_{ij} = b_{0,ij} + b_{1,ij}T + \frac{b_{2,ij}}{T} \tag{12}$$

$$c_{ij} = c_{0,ij} + c_{1,ij}T + \frac{c_{2,ij}}{T} \tag{13}$$

where $b_{ij,\ k}$ (k=0,…,2) and $c_{ij,\ k}$ (k=0,…,2) are adjustable parameters between species i and j that can be obtained by simultaneous inclusion of all available experimental data such as mean activity coefficient, activity of water, osmotic coefficient, heat capacity, and solubility in a single data regression run, and minimization of the differences between the experimental and calculated properties.

Modelling Algorithm

In chemical modelling strategy, the first step is to select a suitable activity coefficient model for the system of interest. Then, equilibrium constants for the system need to be defined and a proper model for the

extrapolation of the equilibrium constants at high temperatures and pressures must be chosen. The next step in chemical modelling is to regress model parameters by using experimental data of the system of interest. Regression of experimental data during chemical modelling ensures thermodynamic consistency among experimental data.

After regression is done and parameter values are obtained, the validation of model parameters is an important step to ensure that regressed parameters produce results consistent with experimental data not used in regression step. This is accomplished by comparing model results with experimental data beyond the range of data used for parameterization. Process modelling without parameter validation can produce serious deviation from experimentally known chemical behavior. Figure 1 shows the chemical modelling algorithm that was used in this work:

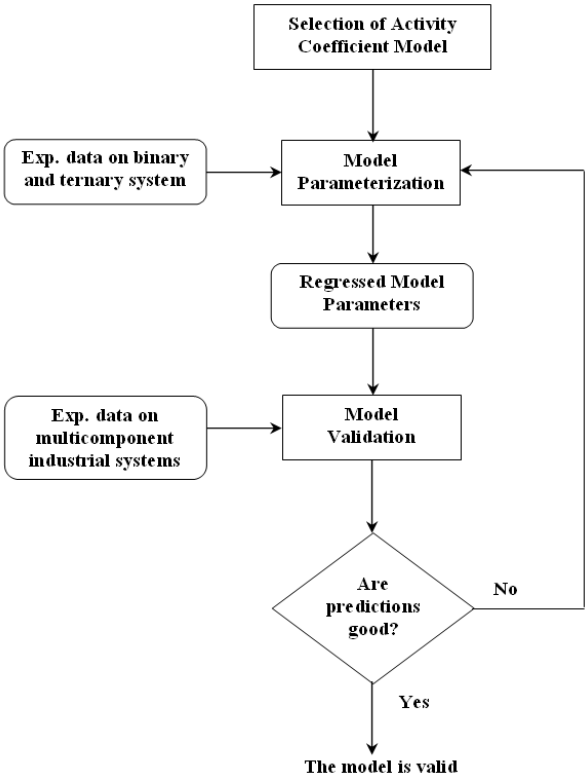

Figure 1 – Chemical modelling algorithm applied in this work

Results and Discussion

Regression of the Model Parameters

A large number of experimental data are available for the solubility of calcium sulphate hydrates in sulphate solutions. In this study, different binary, ternary, quaternary and more complex multicomponent sulphate systems were investigated. Model parameter estimations were performed by the simultaneous inclusion of all available experimental data in a data regression run, and minimization of the differences between the experimental and calculated properties. The validation of the model parameters was made by comparing the model results with experimental data obtained beyond the range of the available data used to determine the parameters.

Fitting Results in Binary and Ternary Systems

$CaSO_4$-H_2O System

The solubility of $CaSO_4$ polymorphs (dihydrate, hemihydrate, and anhydrite) has been extensively measured.[14-23] Most of the measurements are in fairly good agreement with each other. These experimental solubility data were used to verify the OLI default databank. Although the solubility of $CaSO_4$ dihydrate ($CaSO_4.2H_2O_{(s)}$) in H_2O from 0 to 110ºC can be calculated accurately with the MSE OLI default database, there are no data for hemihydrate ($CaSO_4.0.5H_2O_{(s)}$) in the OLI default database. Therefore, literature solubility data[21,22] were used to adjust the standard state Gibbs free energy, the entropy, and the heat capacity of the solid as a function of temperature up to 200ºC. Experimental data on the solubility of anhydrite ($CaSO_{4(s)}$) in water are available and the OLI default database can accurately reproduce all experimental data over a wide temperature range from 0 to 300ºC.

Figure 2 shows the solubility of the three polymorphs of $CaSO_4$. It can be seen that below ~40ºC, $CaSO_4$ dihydrate has the lowest solubility and is therefore the most thermodynamically stable phase. The transition point of $CaSO_4$ dihydrate to anhydrite lies at 40±2ºC, and that of $CaSO_4$ dihydrate to hemihydrate lies at 99±2ºC. In the region between these two temperatures, $CaSO_4$ dihydrate is metastable, although the degree of metastability in dilute aqueous solutions is not significant. Thus, $CaSO_4$ dihydrate-water slurries can be heated to 100ºC without the transformation of $CaSO_4$ dihydrate to anhydrite or hemihydrate.

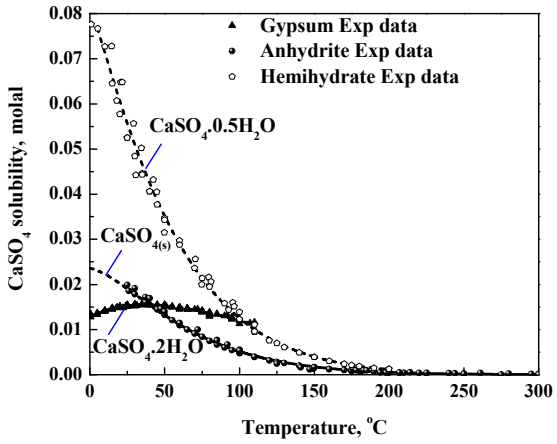

Figure 2 – The solubility diagram of $CaSO_4$ in water; experimental data are from literature[14-23], and the solid and dashed curves show the stable and metastable phases, respectively

$CaSO_4$-H_2SO_4-H_2O System

The solubility of $CaSO_4$ hydrates in H_2SO_4 solutions has been measured by different researchers.[14,24-27] The OLI default database does not predict the solubility behaviour in this system very accurately. Consequently, experimental data for gypsum, hemihydrate and anhydrite were used to regress the MSE middle range interaction parameters between Ca^{2+} and HSO_4^- over a wide temperature range, from 25 to 300ºC. Figure 3 shows the three-dimensional solubility diagram of all three $CaSO_4$ polymorphs in this system. At low temperatures (25-60°C), the addition of H_2SO_4 increases the solubility of $CaSO_4.2H_2O$ moderately, whereas at very high concentrations of acid, the solubility is decreased. At higher temperatures, the solubility increases strongly with increasing acid concentration.

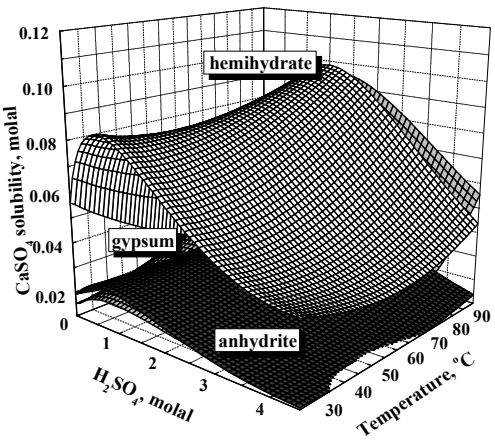

Figure 3 – The phase transition diagram of $CaSO_4$ in H_2SO_4 solutions

$CaSO_4$-$NiSO_4$-H_2O SYSTEM

Campbell and Yanick[28] studied the solubility behaviour of $CaSO_4$ in an aqueous solution of $NiSO_4$ over a temperature range from 45 to 90 ºC. As the OLI default database did not accurately produce these data, model parameters were fitted between Ca^{2+} and Ni^{2+} as well as $CaSO_{4(aq)}$ and Ni^{2+} species in the solution using these data. The fitted model results are shown in Figure 4. As can be seen, model results are in good agreement with experimental data.

As the $NiSO_4$ concentration is increased from pure water, the solubility of $CaSO_4$ initially drops due to the common ion effect (SO_4^{2-} is added) which shifts reaction (1) to the left. However, at around 0.25 molal $NiSO_4$ this effect is cancelled out because of increasing ion interaction or association between Ca^{2+} and SO_4^{2-}. The same behaviour was observed for $CaSO_4$ in other metal sulphates such as $MgSO_4$, $ZnSO_4$, etc.

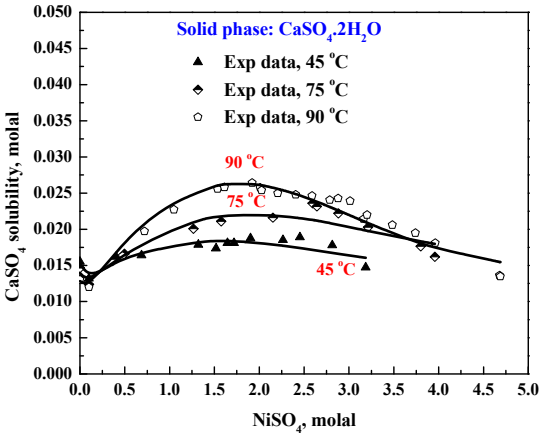

Figure 4 – $CaSO_4$ solubility in $NiSO_4$ solutions; experimental data are from Campbell and Yanick[28], and the curves are the regressed model results

Prediction Results in Multicomponent Solutions

In the previous section, it was shown that the MSE activity model is effective for fitting the solubility of $CaSO_4$ hydrates in binary or ternary electrolyte solutions. In order to validate model parameters, the solubility of

$CaSO_4$ hydrates was calculated in multicomponent aqueous systems containing $NiSO_4$, H_2SO_4, $MnSO_4$, $Fe_2(SO_4)_3$, LiCl, etc. for which no fitting was carried out. As will be seen later in this section, the model is capable of predicting the chemistry of all the multicomponent systems studied. This illustrates the usefulness of the developed model for assessing the scaling potential of calcium sulphate in aqueous processing streams for which no experimental data are available.

$CaSO_4$-$NiSO_4$-H_2SO_4(0.5M)-H_2O System

In nickel hydrometallurgical industries, $NiSO_4$ concentration varies widely as nickel is dissolved from the ore during leaching process or is plated from solution during electrowinning. These variations affect the solubility of calcium sulphate, which is produced during the neutralization of acidic solutions by lime (CaO). The effect of $NiSO_4$ concentration on the solubility of calcium sulphate in solutions containing 0.5M H_2SO_4 as a function of temperature was studied in this work. The solubility of calcium sulphate decreases steadily as the $NiSO_4$ concentration increases from 0.0 to 0.4M $NiSO_4$ because of the common ion effect. In this system, because the acid concentration used is relatively low, the dehydration of gypsum ($CaSO_4.2H_2O_{(s)}$) to anhydrite ($CaSO_{4(s)}$) does not occur at temperatures below 90ºC. Experimental data and model predictions are shown in Figure 5, and it is apparent that the model closely predicts the solution chemistry (AARD%=6), without the need to carry out any additional fitting.

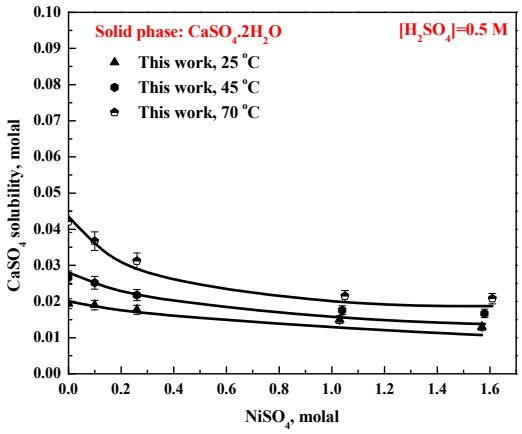

Figure 5 – $CaSO_4$ solubility in $CaSO_4$-$NiSO_4$-H_2SO_4(0.5M)-H_2O solution; experimental data were measured in this work, and curves are predictions

$CaSO_4$-$NiSO_4$ (1.4M)-H_2SO_4(1M)-$Fe_2(SO_4)_3$(0.2M)-LiCl(0.3M)-H_2O System

Nickel processing solutions typically contains $NiSO_4$, H_2SO_4, $Fe_2(SO_4)_3$ and a small amount of a chloride salt. In order to check the predictability of the model in such solutions, the solubility of calcium sulphate dihydrate as a function of temperature was measured in a solution of 1.4M $NiSO_4$, 1M H_2SO_4, 0.2M $Fe_2(SO_4)_3$ and 0.3M LiCl. Solubility measurements were carried out based on heating from 25 to 90°C and subsequent cooling. The results showed that the solubility of calcium sulphate dihydrate increases by increasing temperature up to 70°C. At 70°C, first sample was taken after ~24h which was showing an increase in the solubility by increasing temperature. There was a second sample taken at 70°C after ~72 h for which the solubility was much lower than that of previous sample. Solubility data measured at 90°C had the same order of magnitude as that measured at 70°C after 3 days.

On cooling, a relatively flat solubility curve is noted to 25°C. X-ray diffraction studies of the equilibrating solid phase showed only gypsum during heating up to 70°C and even in the first sample taken at 70°C after 24 hours; however, the solid sample taken at 70°C after 3 days as well as that taken at 90°C show 100% anhydrite in the composition. Hemihydrate was not detected in any of the samples despite a careful search for this phase. On cooling, anhydrite remained the dominant equilibrating solid phase above 25°C, but at 25°C the conversion

of the anhydrite to gypsum occurred. Thus, the major drop in the solubility of calcium sulphate is due to the conversion to anhydrite, a phase which has a significantly different solubility–temperature relationship.

Figure 6 shows these data along with model predicted results. As can be seen, the model can predict the solubility of gypsum and anhydrite precisely. However, the phase transition area, which is not thermodynamically stable, cannot be predicted by the model.

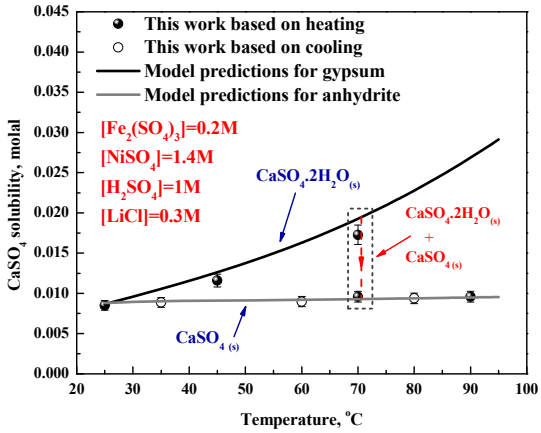

Figure 6 – $CaSO_4$ solubility in $CaSO_4$-$NiSO_4$ (1.4M)-H_2SO_4(1M)-$Fe_2(SO_4)_3$(0.2M)-LiCl(0.3M)-H_2O solution; solid curves are prediction, and dash line shows the phase transition area

$CaSO_4$-$MnSO_4$-H_2SO_4(0.7M)-H_2O System

There are some difficulties involved in the electrolytic process for the winning of manganese dioxide from H_2SO_4/Mn^{2+} electrolyte where $CaSO_4$ scale develops in heat exchangers, pipes and other equipment. These regularly require cleaning to maintain efficient process operation.[29] To study the effect of sulphuric acid, $MnSO_4$ and temperature on the solubility of calcium sulphate hydrates, Farrah et al. [29] measured the solubility of $CaSO_4$ in aqueous solutions containing $MnSO_4$ and H_2SO_4 over the temperature range from 30 to 105°C. Figure 7 shows their experimental solubility data along with the predicted results obtained from the new model.

As is clear in Figure 7, the predicted results obtained from the new model are in very good agreement with experimental data. It is obvious from the figure that gypsum solubility decreases with increasing $MnSO_4$ concentration at fixed H_2SO_4 concentrations due to the common ion effect. On the other hand, there is a regular increase in solubility with temperature in the presence of $MnSO_4$ up to ~80°C because of the tendency of the sulphate ions to form bisulphate ions.

Above 80°C, calcium sulphate solubility declines sharply which is a result of solid phase transformation from gypsum to anhydrite. It can be seen from the figure that the solubility of anhydrite is also depressed by subsequent addition of $MnSO_4$. Temperature appears to have little effect on the solubility.

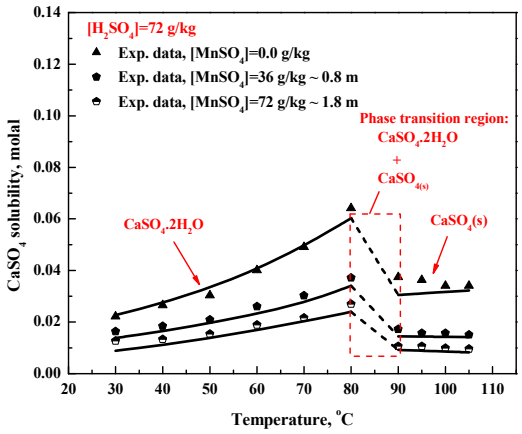

Figure 7 – $CaSO_4$ solubility vs. temperature in $CaSO_4$-$MnSO_4$-H_2SO_4-H_2O solutions; the experimental data are from Farrah et al.[29]; the solid curves are the predicted values and the dashed lines show the phase transition region

Conclusions

The solubility of calcium sulphate hydrates was successfully modelled using the Mixed Solvent Electrolyte model via OLI software. Modelling involved the fitting of binary activity, heat capacity, and solubility data as well as ternary solubility data. New interaction parameters for calcium ions and associated calcium sulphate neutral species with other dominant species in the solution were determined. The model can be used to assess the calcium sulphate scaling potential in different processes over a wide range of temperature and ionic strength.

In hydrometallurgical processing of metals such as copper, manganese and nickel, the limited solubility of calcium sulphate results in very low concentration of calcium in the circuit. However, as temperature and solution composition vary, calcium sulphate scaling may occur elsewhere in the process.

As well, at higher temperatures transformation between the calcium sulphate polymorphs can have a complex effect on solubility, making the behaviour of calcium sulphate difficult to predict and control. Most of the industries which are involved with calcium sulphate scale formation need regular removal of precipitated calcium sulphate hydrates since the build-up in calcium concentration in these process streams are unavoidable.

The model was shown to accurately predict the solubility behaviour of calcium sulphate in solutions containing $NiSO_4$, H_2SO_4, $Fe_2(SO_4)_3$, and LiCl, from room temperature to 90ºC. The solubility of calcium sulphate in water reaches a maximum at around 40ºC, followed by a slight decrease in the solubility at higher temperatures. The addition of H_2SO_4 results in a significant increase in the calcium sulphate solubility. By increasing the acid concentration, gypsum dehydrates to anhydrite. This conversion results in a decrease in the solubility of calcium sulphate in the solution.

As a result of the above, process solutions operating under atmospheric pressure which are saturated with calcium sulphate during an upstream neutralization step have the potential for gypsum scale formation when cooled. Gypsum scale formation occurs because gypsum solubility decreases upon cooling.

As it is not practical to measure solubility data under all possible conditions, because of the large number of components involved, chemical modelling becomes a valuable tool for assessing the solubility of calcium sulphate in various aqueous processing streams.

Acknowledgments

The authors would like to acknowledge the financial support provided by Vale Inco Ltd. and the Natural Sciences and Engineering Research Council of Canada (NSERC) for this project.

Literature Cited:

1. Hasson D. Precipitation fouling: fouling of heat transfer equipment. Washington: Hemisphere Publishing Corp., 1981.
2. Adams JF. Gypsum scale formation and control during continuous sulphuric acid neutralization. University of Toronto: Ph.D. thesis, 2004.
3. Marshall W, Slusher R. Thermodynamics of calcium sulfate dihydrate in aqueous sodium chloride solutions, 0-110 ºC. Journal of Physical Chemistry. 1966; 70: 4015-4027.
4. Marshall W, Slusher R. Aqueous systems at high temperature, solubility to 200 ºC of calcium sulphate and its hydrates in seawater and saline water concentrates, and temperature-concentration limits. Journal of Chemical and Engineering Data. 1968; 13: 83-93.
5. Tanji KK, Doneen LD. Predictions on the solubility of gypsum in aqueous salt solutions. Water Resources Research. 1966; 2: 543-548.
6. Barba D, Brandani V, Giacomo G. A Thermodynamic model of $CaSO_4$ solubility in multi-component aqueous solutions. The Chemical Engineering Journal. 1982; 24: 191-200.
7. Zemaitis JF, Clark DM, Rafal M, Scrivner NC. Handbook of aqueous electrolyte thermodynamics theory and Application. AICHE: New York, 1986.
8. Arslan A, Dutt GR. Solubility of gypsum and its prediction in aqueous solutions of mixed electrolytes. Soil Science. 1993; 155: 37-47.
9. Li Z, Demopoulos GP. Development of an improved chemical model for the estimation of $CaSO_4$ solubilities in the HCl-$CaCl_2$-H_2O system up to 100 ºC. Industrial and Engineering Chemistry Research. 2006; 45: 2914-2922.
10. Li Z, Demopoulos GP. Speciation-based chemical equilibrium model of $CaSO_4$ solubility in the H + Na + Ca + Mg + Al + Fe(II) + Cl + H_2O system. Industrial and Engineering Chemistry Research. 2007; 46: 6385-6392.
11. Wang P, Anderko A, Young RD. A speciation-based model for mixed-solvent electrolyte systems. Fluid Phase Equilibria. 2002; 203: 141–176.
12. Wang P, Springer RD, Anderko A, Young RD. Modeling phase equilibria and speciation in mixed-solvent electrolyte systems. Fluid Phase Equilibria. 2004; 222–223: 11–17.
13. Wang P, Anderko A, Springer RD, Young RD. Modeling phase equilibria and speciation in mixed-solvent electrolyte systems: II. Liquid–liquid equilibria and properties of associating electrolyte solutions. Journal of Molecular Liquids. 2006; 125: 37-44.
14. Dutrizac JE, Kuiper A. The solubility of calcium sulphate in simulated nickel sulphate-chloride processing solutions. Hydrometallurgy. 2006; 82: 13-31.
15. Tanger IV JC, Helgeson HC. Calculation of the thermodynamic and transport properties of aqueous species at high pressures and temperatures: revised equations of state for the "HKF" standard partial molal properties of ions and electrolytes. The American of Journal of Science. 1988; 288: 19-98.
16. Azimi G, Papangelakis VG, Dutrizac JE. Modelling of calcium sulphate solubility in concentrated multi-component sulphate solutions. Fluid Phase Equilibria. 2007; 260: 300-315.
17. Pitzer KS. Electrolytes, from dilute solutions to fused salts. Journal of American Chemical Society. 1980; 102: 2902-2906.
18. Hill AE, Wills JH. Ternary systems. XXIV. calcium sulfate, sodium sulfate and water. Journal of the American Chemical Society. 1938; 60: 1647-1655.
19. Posnjak E. The System $CaSO_4$ - H_2O. American Journal of Science. 1938; 35A: 247-272.
20. Marshall WL, Slusher R, Jones EV. Aqueous systems at high temperature, XIV. solubility and thermodynamic relationships for $CaSO_4$ in NaCl-H_2SO_4 solutions from 40 to 200ºC., 0 to 4 molal NaCl. Journal of Chemical and Engineering Data. 1964; 9: 187-191.
21. Partridge EP, White AH. The solubility of calcium sulfate from 0 to 200ºC. Journal of the American Chemical Society. 1929; 51: 360-370.
22. Sborgi U, Bianchi C. The solubilities, conductivities and X-ray analyses of anhydrous and semihydrated calcium sulphate. Gazzetta Chimica Italiana. 1940; 70: 823-835.
23. Straub FG. Solubility of calcium sulfate and calcium carbonate at temperatures between 182 and 316ºC. Industrial and Engineering Chemistry. 1932; 24: 914-917.
24. Ling Y, Demopoulos GP. Solubility of calcium sulphate hydrates in (0 to 3.5) $mol.kg^{-1}$ sulphuric acid solutions at 100ºC. Journal of Chemical and Engineering Data. 2004; 49: 1263-1268.

25. Zdanovskii AB, Vlasov GA. Determination of the boundaries of the reciprocal transformation of $CaSO_4.2H_2O$ and γ-$CaSO_4$ in H_2SO_4 solutions. Russian Journal of Inorganic Chemistry. 1968; 13: 1318-1319.
26. Zdanovskii AB, Vlasov GA, Sotnikova LI. Dehydration of gypsum in sulfuric acid solutions. Russian Journal of Inorganic Chemistry. 1968; 13: 1418-1420.
27. Marshall WL, Jones EV. Second dissociation of sulphuric acid from 25 to 350ºC evaluated from solubilities of calcium sulphate in sulphuric acid solutions. The Journal of Physical Chemistry. 1966; 70: 4028-4040.
28. Campbell AN, Yanick NS. The System $NiSO_4$-$CaSO_4$-H_2O. Transactions of the Faraday Society. 1932; 28: 657-661.
29. Farrah HE, Lawrance GA, Wanless EJ. Solubility of calcium sulphate Salts in acidic manganese sulphate solutions from 30 to 105 °C. Hydrometallurgy. 2007; 86: 13-21.